ELSEVIER

Journal of Alloys and Compounds 320 (2001) 282–295

Journal of ALLOYS AND COMPOUNDS

www.elsevier.com/locate/jallcom

Prediction of the distribution of alkali and trace elements between the condensed and gaseous phases generated during clinical waste incineration

I. Delay[a,*], J. Swithenbank[b], B.B. Argent[c]

[a]*Airbus UK Ltd., New Filton House, Filton, Bristol BS 99 7AR, UK*
[b]*Department of Chemical Engineering and Process Engineering, University of Sheffield, Sheffield, UK*
[c]*Department of Engineering Materials, University of Sheffield, Sheffield, UK*

Abstract

The mobilisation of alkali and trace elements present in clinical waste can lead to accelerated deterioration of the plant and to environmental damage. The damage can be caused by transfer of low levels of trace elements, which are difficult to monitor, and a model of the underlying processes which predicts the degree of mobilisation of each element from waste of specified characteristics is thus desirable. The Equilibrium module of the FACT suite of computer programs has been used to make predictions for alkali and trace element mobilisation from a typical waste composition with variation in the S/Cl ratio which influences the volatilisation/condensation processes. Although thermodynamic data for some of the potential melts are incomplete, predictions made using the various oxide melt models, matte, salt and solid solution models available in FACT are combined to allow meaningful comment on Pb, Cu, Zn, Ni and Cr distributions. Separate consideration is given to mobilisation in primary (pyrolysis) and secondary combustion (oxidation) chambers. Comparisons are made with published data from municipal waste incineration plants. An interesting feature of the predictions for condensation during cooling of the waste gases is that if solution of Pb, Zn and Cu chlorides is permitted in alkali chloride or Pb sulphate into sulphate melts then Pb and Cu are predicted to be largely removed from the gas stream into these melts.

Keywords: Alkali; Trace elements; Clinical waste incineration

1. Introduction

Incineration has been recognised by governmental bodies as an acceptable method of disposal for all clinical waste, and it is the only suitable route for certain waste arisings such as human residues and potentially infectious wastes. However, recognition of the potential environmental problems generated by burning wastes has a long history. The release into the environment of by-products of the incineration process, in particular ash residues containing trace elements, such as As, Hg, Ni, Cr, Cd or Pb known for their cumulative toxicological effects, has always been a source of concern. An improved understanding of the transport mechanisms of such elements in incineration is needed to identify the potential problems associated with their release/disposal in the environment.

*Corresponding author. University of Surrey, Centre for Environmental Strategy, Guildford GU2 5HX, UK.

2. An overview of the transport mechanisms

There has been much speculation as to the mechanisms involved in the formation of metal-containing compounds in waste combustion ash. A formation mechanism, referred to as the volatilisation–condensation theory has been widely accepted with modifications, to partially explain the transport of heavy metals during both coal and municipal waste combustion [1,2]. This theory led to a classification of elements according to their boiling points as this was demonstrated by Davison et al. [1] to be the primary factor that determines when a metal is present in the matrix of the fly ash particles or on their surface. This classification is given in Table 1.

Identification of spatial distributions, morphologies, and chemical compositions is necessary to understand the fate and transport of heavy metals. The key objective is to determine the likely location and form of toxic elements present at significant concentrations in the fly-ash particles,

0925-8388/01/$ – see front matter
PII: S0925-8388(00)01479-1

Table 1

Class I	Al, Ba, Be, Ca, Co, Fe, K, Mg, Si, Sr, Ti	High boiling points Mainly in fly-ash matrix Minimum deposition at the surface
Class II	As, Cd, Cu, Ga, Pb, Sb, Zn and Se	Volatilisation-gas phase Minimum presence in bottom ash Condensation on fly-ash particle surface while gas stream cooling down
Class III	Hg, Cl and Br	Low boiling points Volatilisation Remain in gas phase through the entire process

bearing in mind that elements at the surface have more chances to leach and to pose environmental and safety problems.

Among the numerous factors to be considered in this problem, design parameters particularly temperature and residence time, oxidative or reductive conditions together with the waste composition are of primary importance. The interaction between the volatilisation of heavy metals and the presence of HCl and SO_2 in combustion gases has already been noted. Greenberg et al. [3] stated that a possible effect of high concentrations of chlorine compounds in the combustion gas stream may be the formation of chlorides of Pb, Sb, Cd, As, Zn, and Ni, whose boiling points are below 1273 K (954°C for Pb, 283°C for Sb, 960°C for Cd, 130°C for As, 732°C for Zn, 973°C for Ni). They found Cl concentrations of 14–20% sufficient to supply anions for many of the metals present. However, other observations like the absence of Fe and Al chlorides on the outside of particles led them to think that the full explanation was more complicated. Both experimental observations and theoretical studies are needed to provide definite conclusions.

2.1. Equilibrium predictions

Research conducted by Fernandez et al. [4] included evaluation of possible metal compounds based on available thermochemical data. They determined the free energies of formation of chlorides and oxides to predict which one was thermodynamically favourable. They indicated that lead chloride formation was favoured over lead oxide formation over a wide range of temperatures and concluded that when the chloride became more stable than the oxide, the heavy metal is transported as a chloride by volatilisation-condensation, resulting in heavy metal deposition on the surface of fly-ash particles and high solubility compounds. Wu and Biswas [5] performed an equilibrium analysis of the speciation of six metals among various species in an incinerator system according to temperature and chlorine content. They showed that Hg and Cd could be expected to remain in their elemental form, chromium would form hydroxide species, lead and arsenic would preferentially be found in chloride compounds and tin in oxides. These results however relate only to the volatilisation stage and do not give any indication of the condensed metal phases. Moreover the potential sulphur content in the gas phase was not included in the equilibrium analysis eliminating therefore the possible formation of sulphates over chlorides.

2.2. Experimental observations

A comprehensive study was made by Eighmy et al. [6] to characterise speciation of major, minor and trace elements in electrostatic precipitator (ESP) ash from a municipal solid waste incinerator. Different analytical techniques were used to quantify elements, describe particles and phase associations, identify bulk and surface mineral phases, and identify the speciation of elements. The mineralogy was determined by X-ray powder diffraction (XRPD) and scanning electron microscopy/energy dispersive spectrometry (SEM/EDS). A wide variety of compounds containing Pb (K_4PbO_4, Pb_3SiO_5, $Pb_3S_2O_7$, $PbSO_4$), Zn (K_2ZnCl_4) and Cd ($Cd_5(AsO_4)_3Cl$) were identified as probable minerals. Some of the minerals are similar to the ones observed by Hundesrugge et al. [7] such as SiO_2, NaCl, KCl, $CaSO_4$, glass and carbon particulate and by Ontiveros et al. [8] who also found Fe_3O_4 and Fe_2O_3.

X-ray photoelectron spectroscopy (XPS) was used as a surface technique to provide information on speciation at the particle surface. For major elements such as Cl, Na and K, the species identified included alkali chlorides, metal sulphates and various oxides. A number of interesting phases were found for zinc and lead, chloride compounds ($ZnCl_2$ and $PbCl_2$) appearing to be dominant over oxides, sulphates and elemental forms. Clinical incinerator ash has also been tested for leachability purposes through the Coalition on Resource Recovery and the Environment (CORRE) and was found to be rich in chlorides and sulphates [9]. Research studies by Sandell et al. [10] focused on composition, morphology, and distribution of lead bearing phases in municipal solid waste combustor fly-ash. Using SEM/EDS and digital imaging software, they observed lead in two forms — Pb–Cl rich inclusions that exhibit no specific crystal habit, and in lower concentration, K–Cl–Pb and Na–Cl–Pb inclusions that exhibit a cubic habit. They emphasised that lead is present at

Table 2
Typical clinical waste composition

Composition	Clinical waste wt. (%)
Paper	34.50
Plastic	22.70
Fluids	12.24
Food	8.49
Metals	5.37
Rubber	4.58
Glass	4.32
Textiles	2.97
Cardboard	2.10
Yard waste	1.40
Misc. organics	1.33
Total	100.00

the surface of the particles and in the interior, challenging volatilisation-condensation as the main mechanism for lead transport and lead's classification as either a class I or II element.

3. Thermodynamic modelling

3.1. Clinical waste composition

Clinical waste is defined as all waste generated from health related activities. A literature survey has been carried out to derive a good estimate of the weight contribution of major components (paper, plastics, glass . . .) in the clinical waste stream. A typical waste composition adapted from Hasselriis [11] is given in Table 2. Paper and plastics contribute together more than 50% of the clinical waste weight. This is particularly interesting as paper and plastics are both sources of metals. Cr, Pb and Fe are used in printing inks; Ba, Cd, Pb, Zn and Sr all belong to the range of metals used as stabilisers in plastics; Cd, Ni, Zn and Cr are found in colorants. Pb is one of the most common stabilisers found in PVC and Polyethylene [12]. In order to establish typical elemental compositions for clinical waste, a thorough review of the composition of the main components (paper, glass, textile) including the different types for plastics, potential presence of trace elements (metals, alkalis), and representative elemental composition of the human body and food was carried out. The typical elemental compositions varying in S, Cl and alkali content resulting are given in Table 3. Twenty-four elements is the maximum allowed by the FACT [13] program used for modelling. The 24 elements were chosen on the basis of their importance and on the availability of thermodynamic data.

3.2. Plant conditions

In order to simulate the combustion of clinical waste in the incinerator, our calculations were divided in three

Table 3
Typical elemental compositions

Code	1	2	3	4	5	6	7	8
S/Cl mole ratio	0.1228	0.1228	0.2211	0.3365	0.5528	0.5528	0.5528	0.5528
Na+K	0.0476	0.0780	0.0780	0.0780	0.0780	0.0691	0.0563	0.0476
				wt.%				
Al	0.90	0.90	0.90	0.90	0.90	0.90	0.90	0.90
Ba	0.20	0.20	0.20	0.20	0.20	0.20	0.20	0.20
C	39.50	39.50	39.50	39.50	39.50	39.50	39.50	39.50
Ca	1.50	1.50	1.50	1.50	1.50	1.50	1.50	1.50
Cd	0.05	0.05	0.05	0.05	0.05	0.05	0.05	0.05
Cl	2.70	2.70	2.50	2.30	2.00	2.00	2.00	2.00
Cr	0.15	0.15	0.15	0.15	0.15	0.15	0.15	0.15
Cu	0.05	0.05	0.05	0.05	0.05	0.05	0.05	0.05
Fe	4.30	4.30	4.30	4.30	4.30	4.30	4.30	4.30
H	7.00	7.00	7.00	7.00	7.00	7.00	7.00	7.00
Hg	0.05	0.05	0.05	0.05	0.05	0.05	0.05	0.05
K	0.50	0.50	0.50	0.50	0.50	0.50	0.50	0.50
Mg	0.30	0.30	0.30	0.30	0.30	0.30	0.30	0.30
N	0.60	0.60	0.60	0.60	0.60	0.60	0.60	0.60
Na	0.80	1.50	1.50	1.50	1.50	1.00	1.00	0.80
Ni	0.05	0.05	0.05	0.05	0.05	0.05	0.05	0.05
O	37.00	37.00	37.00	37.00	37.00	37.00	37.00	37.00
P	0.20	0.20	0.20	0.20	0.20	0.20	0.20	0.20
Pb	0.20	0.20	0.20	0.20	0.20	0.20	0.20	0.20
S	0.30	0.30	0.50	0.70	1.00	1.00	1.00	1.00
Si	2.90	2.20	2.20	2.20	2.20	2.20	2.70	2.90
Sn	0.05	0.05	0.05	0.05	0.05	0.05	0.05	0.05
Ti	0.50	0.50	0.50	0.50	0.50	0.50	0.50	0.50
Zn	0.05	0.05	0.05	0.05	0.05	0.05	0.05	0.05

distinct phases based on the incineration process stages. The first stage represents the pyrolysis and gasification of the waste in the primary combustion chamber at 900°C, the gas phase is then oxidised with 5–10% excess air (calculations were undertaken with a free O_2 concentration of 6.3 vol.%) at 1025°C simulating the combustion in the secondary chamber. The flue gases are finally cooled down to ~325°C or to ~100°C which correspond, respectively to the typical temperatures found at the boiler exit and in the flue gas treatment system.

For each computation the reactants are waste input elements (Table 3) for the first stage, and elements carried forward in the gas phase in the next stages, which means that the material present in compounds present in liquid solutions or solid species at 1298 K is not considered during gas cooling. The final states correspond to a pressure of 1 atm. (101.325 kN/m^2) and the final temperatures. (These are 1173, 1298, 600 and 375 K, with 1000 and 800 K added to highlight the formation of fused salt melts).

3.3. Thermodynamic package: FACT

The equilibrium module of the FACT suite of computer programs has been used to make predictions for alkali and trace element mobilisation based on typical waste compositions. This exercise included variation in the S/Cl ratio of the waste and the alkali content which were recognised to be influencing factors during the volatilisation/condensation processes. Facility for the analysis of chemical thermodynamics (FACT) is a computational package which performs a wide range of thermodynamics calculations based upon a comprehensive thermochemical database. It consists of a number of modules which permit modification of substance and solution databases as well as computing the equilibria for specific analyses at a defined temperature and pressure. The calculation is based on the minimisation of the system's Gibbs free energy for different possible phase assemblages. The main reason for choosing FACT was that the solution data base for silicate melts covers a wider range of components than is openly available from its principal competitors and there are additional databases related to fused salt and sulphide melts.

The predictions presented in this paper were made with the new Windows version of FACT. This has revised and expanded databases. In practice, with the elements relevant to potential environmental problems associated with incineration there is a practical limit of about 18 elemental components and 10–14 slag forming species. The slag database permits the combination of slag-forming components CaO, Al_2O_3, SiO_2, FeO, Fe_2O_3, Na_2O, K_2O, MgO, phosphate, TiO_2 and Ti_2O_3 with sulphides, sulphates, Mn, Cr, Ni, Pb, Cu, Zn and As. However, the database is not optimised for all combinations. Slag analyses from preliminary calculations made allowing formation of a matte, salt melt, melilite and spinel solutions and a slag based on CaO, Al_2O_3, SiO_2, FeO, Fe_2O_3, Na_2O, K_2O, MgO, TiO_2, Ti_2O_3 with sulphates, sulphides and chlorides of sodium, potassium, magnesium and calcium are given in Table 4.

Under pyrolysis conditions the equilibrium distribution would place roughly 60% of the chlorine in the gas phase, 3–4% in the slag and the remainder in the mixed chloride/sulphate melt. The sulphur distribution depends on whether a sulphide melt is formed. This occurs with high sulphur contents and then roughly 60% of the sulphur would be in the sulphide melt, very small amounts in the slag and salt melts and the remainder in the gas phase. With low sulphur contents a sulphide melt is not formed and over 99% of the sulphur is in the gas phase. Under combustion conditions, more than 97% of the chlorine is in the gas phase with small amounts in the slag and molten salt phases. Subsequently, 48–49% of the sulphur is in the gas phase and the remainder distributed between slag and fused salt melt. With the practical restriction on the number of slag species that can be considered it is necessary to decide whether to allow sulphate species in the slag formed under combustion conditions; sulphide and chloride species can obviously be ignored. Equilibrium between a sulphur-rich gas phase and a slag melt is unlikely in view of the low diffusion coefficients (D) reported for silicate melts at 1000°C ($D \approx 1\times10^{-9}$) and the short gas residence times which are less than 10 s. It was therefore decided not to permit the solution of sulphate species in the slag and to instead consider a greater number of trace elements.

A second series of tests with titanium showed that less than 1×10^{-9} mol.% was in the gas phase and that when a slag phase was present approximately 47 mol.% was in the slag — corresponding to 3.8 wt.% TiO_2 in the slag — and 53 mol.% in $CaTiO_3$. Consequently it was decided not to include titanium in the slag as it only served to confirm how little could be volatilised. Thus the chosen slag matrix was CaO, Al_2O_3, SiO_2, FeO, Fe_2O_3, Na_2O, K_2O and MgO. As and Mn were ignored as their concentrations were $<$0.01 wt.%. Ba, Cd, Hg and Sn were not included in the solution-slag database and were therefore considered on the basis of their stoichiometric compounds. Two combinations of trace elements were used for each base composition Cd, Cu, P, Pb, and Zn — with Cu, P, Pb and Zn entering the slag phase (a series) or Ba, Cr, Hg, Ni, Sn and Ti with only Cr and Ni being considered in the slag (c series). These combinations are not fully optimised subsets of the database, but it is considered that the advantages of having realistic slag volumes at the temperature of the combustion chamber outweigh the disadvantages at low trace element concentrations. The use of two separate combinations was a consequence of the practical limitations of the software.

The results from the pairs of calculations were combined for the cooling calculations which were carried out in the DOS version of FACT using the 20 element combination

Table 4

(a) Slag analyses showing distribution of sulphur and chlorine

	Pyrolysis (1173 K)				Combustion (1298 K)			
Code	1c	2c	5c	8c	1c	2c	5c	8c
Mole ratio S/Cl	0.1229	0.1229	0.5528	0.5528	0.1229	0.1229	0.5528	0.5528
Moles Na+K	0.0476	0.0780	0.0780	0.0476	0.0476	0.0780	0.0780	0.0476
g. slag	6.1347	7.8396	8.9578	6.5989	10.2520	10.6520	10.8410	10.404
Component	Wt.% component							
Al_2O_3	15.56	19.56	18.17	16.12	15.92	15.96	15.69	15.34
CaO	13.20	12.18	12.37	13.95	15.67	11.83	11.42	15.23
K_2O	1.24	0.49	0.98	1.19	1.28	1.25	1.06	1.58
MgO	1.38	3.51	3.29	1.49	3.10	4.37	4.08	3.02
Na_2O	9.98	11.33	12.11	10.38	8.57	12.36	10.66	8.69
SiO_2	54.68	47.65	48.50	53.07	51.31	44.18	43.41	51.23
TiO_2	1.48	3.66	3.10	1.66	3.75	5.05	5.52	3.65
Ti_2O_3	1.09E-04	4.01E-04	2.24E-04	1.07E-04	1.21E-07	5.51E-08	8.53E-08	1.03E-07
CaS	2.58E-03	5.90E-03	9.33E-03	5.36E-03	1.19E-20	4.70E-21	1.06E-20	3.68E-20
K_2S	2.20E-04	2.17E-04	6.75E-04	4.15E-04	8.87E-22	4.53E-22	8.97E-22	3.46E-21
MgS	2.94E-04	1.85E-03	2.70E-03	6.21E-04	2.57E-21	1.88E-21	4.12E-21	7.93E-21
Na_2S	1.91E-03	5.37E-03	8.94E-03	3.90E-03	6.39E-21	4.80E-21	9.68E-21	2.05E-20
$CaSO_4$	2.89E-17	2.97E-17	6.39E-17	5.66E-17	0.19	1.89	3.36	0.66
K_2SO_4	2.06E-18	9.15E-19	3.87E-18	3.67E-18	1.21E-02	0.1529	0.2384	5.18E-02
$MgSO_4$	3.71E-18	1.05E-17	2.09E-17	7.42E-18	0.05	0.86	1.48	0.16
Na_2SO_4	2.06E-17	2.61E-17	5.90E-17	3.97E-17	0.10	1.87	2.96	0.35
$CaCl_2$	1.30	0.71	0.63	1.12	2.87E-02	8.57E-02	4.91E-02	1.80E-03
KCl	9.72E-02	2.31E-02	4.02E-02	7.61E-02	1.88E-03	7.27E-03	3.66E-03	1.80E-03
$MgCl_2$	0.16	0.25	0.20	0.14	6.78E-03	3.77E-02	2.10E-02	5.15E-03
NaCl	0.9342	0.6340	0.5893	0.7935	1.50E-02	8.53E-02	4.37E-02	1.18E-02

(b) Slag analyses showing effect of S/Cl ratio and alkali content on trace element levels

Code	1a	1c	2a	2c	5a	5c	8a	8c
g slag at 1298 K	9.4158	9.2484	10.0390	9.6898	10.1730	9.8288	9.4721	9.3948
Mole ratio S/Cl	0.1228	0.1228	0.1228	0.1228	0.5528	0.5528	0.5528	0.5528
Moles Na+K	0.0476	0.0476	0.0780	0.0780	0.0780	0.0780	0.0476	0.0476
Component	Wt.% in slag							
Al_2O_3	15.59	16.83	16.94	17.55	16.72	17.30	15.37	16.25
CaO	12.14	14.83	15.99	15.62	15.85	15.40	12.16	14.45
CrO	–	1.87E-05	–	1.03E-05	–	8.47E-06		1.63E-05
Cr_2O_3	–	2.01E-04	–	1.17E-04	–	8.59E-05		1.51E-04
Cu_2O	8.71E-02	–	0.14	–	0.18	–	0.11	
FeO	8.74E-02	9.10E-02	7.10E-02	6.76E-02	6.45E-02	5.78E-02	8.10E-02	7.98E-02
Fe_2O_3	4.55E-03	5.60E-03	5.52E-03	4.55E-03	4.80E-03	3.50E-03	4.00E-03	4.18E-03
K_2O	1.38	1.27	0.86	0.98	1.12	1.36	1.58	1.62
MgO	4.02	3.65	4.82	4.53	4.74	4.47	4.03	3.48
Na_2O	9.26	9.26	12.11	12.66	12.54	13.51	9.50	9.53
NiO	–	2.21E-02	–	1.93E-02	–	1.65E-02		1.86E-02
PbO	7.22E-02	–	7.51E-02	–	1.23E-01	–	1.19E-01	
SiO_2	56.46	54.05	46.89	48.57	46.26	47.89	55.98	54.58
TiO_2	–	–	–	–	–	–	–	–
Ti_2O_3	–	–	–	–	–	–	–	–
ZnO	0.28	–	0.39	–	0.49	–	0.38	–
$Ca_3(PO_4)_2$	0.30	–	0.82	–	0.91	–	0.32	–
$Mg_3(PO_4)_2$	0.12	–	0.29	–	0.32	–	0.12	–
$Na_3(PO_4)$	0.22	–	0.60	–	0.69	–	0.24	–

Ba, C, Ca, Cd, Cl, Cr, Cu, Fe, H, Hg, K, Mg, N, Na, Ni, O, Pb, S, Sn and Zn. Al, Si, P, Ti, were excluded due to the small amounts volatilised. Only the amounts of Ba, Cr, Hg, Ni, Sn and Ti were taken from the second set of calculations. For most of the elements common to both sets of calculations, this will only lead to small increases in uncertainty. However, if barium has time to form the equilibrium amount of $BaSO_4$ in the combustion stage this will lead to an overestimate of the amount of sulphur carried forward to the gas cooling stages of 5–16%; the error being greatest for low amounts of sulphur in the charge. It is felt that the procedure used, although limited by missing data and constraints of the current software, gives a reasonable basis for examining the mobilisation and final distribution of a number of the elements considered potentially harmful.

4. Results and discussion

4.1. Pyrolysis and oxidation stages

Table 5 shows the distribution of the elements between the gas, liquid and solid phases for both pyrolysis at 1173 K and combustion with approximately 6.3% of O_2 ⟨g⟩ at 1298 K. Greater detail of the speciation is given in Table 6.

Under pyrolysis conditions only small amounts of the following elements are volatilised: Al, Ca, Fe, Mg, Si, Ti, Ba, P, Cr, Cu and Ni. In the case of Sn, SnS is the principal gas, and although for low sulphur contents only about 10% of the Sn is in the gas phase at high sulphur contents this can be more than 98%. Cd, Hg and Zn, H, N, O, are largely in the gas phase whereas Na, K, C, Cl have significant amounts in both the gas and condensed phases. Sulphur is largely volatilised at low S contents but is concentrated in the matte at high S contents.

Under combustion conditions most of the C, H, N, O, Cl, S, K, Cd, Cu, Hg, Pb is volatilised whilst Cr, Ni, Sn, Al, Ca, Fe, Mg, Si, Ti and Ba tend to remain in condensed phases. These results agree fairly well with the theoretical classification of elements and their transport behaviour given earlier. Figs. 1 and 2 emphasise how greater quantities of the trace elements are volatilised at low S/Cl ratios and how competition by Na and K for Cl causes the volatilisation of Cu and Zn to decrease with increasing alkali content.

Pyrolysis takes place with low oxygen contents and the melt system includes sulphides as well as slag and molten salt. The gas phase is dominated by N_2, CO, HCl and H_2S. The behaviour of some metals, most notably Cu and Ni, is changing too, with in this case, a strong reduction of Cu and Ni vaporisation in favour of Cu and Ni presence in matte. The formation of a range of different solid species is predicted, including minerals such as $BaCl_2$, $CaAl_2Si_2O_8$, Ca_3PO_4, $CaTiO_3$, $KAlSi_2O_6$, $MgO.CaO.Si_2O_4$ and $MgO.Cr_2O_3$, as well as metallic compounds such as Fe_3C, Fe_2P, and Ni_3Sn_2. Not too much emphasis should be given to the results obtained for the pyrolysis stage, as a small addition of air is anyway required in the bed during the burn down phase to minimise residual carbon.

Under combustion conditions around 1300 K, the gas phase is dominated by N_2, H_2O, CO_2, O_2, SO_2 and HCl as the main gas compounds. The programme also predicts the formation of a slag for which the composition varies as a function of the S/Cl ratio. Details of the slag analyses are given in Table 4. The presence of slag at 1298 K gives the possibility of heavy metals such as Pb, Zn, Ni, Cr, Cu present in the gas phase to be sequestered in the glassy phase formed from the slag. The entry of the trace elements into the oxides melts will be mainly controlled by the diffusion coefficients and the solubility of the metal compounds. Among the solid compounds present at this stage are Fe_2O_3, $Ca_3(PO_4)_2$, $MgO.Cr_2O_3$, $CaTiO_3$, $CaSiTiO_5$, $NiO.Fe_2O_3$ and $BaSO_4$.

4.2. Condensation stages

The cooling of the flue gas, carried over from the oxidation stage from 1250 to 375 K, leads as expected to the removal of most heavy metals (except Hg) originally present in the gas phase, forming oxides, chlorides or sulphates. Figs. 3–6 show the percentage of various elements present in the gas leaving the combustion chamber after cooling to 1250, 1000, 800, 600 and 375 K. Two different charge compositions coded as 5 (S/Cl= 0.5528) and 2 (S/Cl=0.1228) are shown with two diagrams for each composition to separate the behaviour of the elements. Lower trace element levels in the gas phase are predicted at each temperature for the high S/Cl charge. Examination of Table 7 shows the higher temperatures at which condensation of each species occurs when the S/Cl ratio is high and the complexity possible in the condensation sequence. (Note: no attempt has been made to model the reagents added for gas clean up purposes.)

The heavy and alkali metals particulates are likely to condense on the surface of fly-ash particles entrained from the combustion stages. Although glassy materials are dominant in the fly-ash matrix, minerals initially present in the waste input and not destroyed during the process can also be present.

The salt solutions considered in the cooling calculations were restricted to the alkalis and Table 8 shows how the proportion of sulphates increases, as expected, with S/Cl ratio. The precipitation of trace element sulphates and chlorides indicated in Table 7 suggests that the solution of trace elements in the alkali salt melts should also be considered. Unfortunately, many sulphates decompose before melting and therefore thermodynamic data for the molten trace element sulphates are generally not available. Nevertheless, phase diagrams for the relevant systems show that solution of trace element species occurs in the molten alkali sulphates. Data were found for the solution of copper, zinc and lead chlorides in alkali chlorides [15] and calculations on the cooling of composition code 2, which gave high chloride contents in the salt melt using these showed the potential significance of these solutions in condensing out the trace elements (Table 9). Thermodynamic information is available for molten lead sulphate and use of a simple ideal solution model containing $MgSO_4$, $CaSO_4$, Na_2SO_4, K_2SO_4 and $PbSO_4$ shows that at 1000 K, 63% of the Pb originally in the gas phase may be dissolved in the sulphate solution. From these calculations we conclude that if appropriate data were available for the solution of trace element species in the mixed alkali sulphate and chloride melts significant condensation of the trace element species would be predicted at higher temperatures.

4.3. Trace metal speciation

The speciation of trace metals across the range of temperature studied is summarised in Tables 5 and 6 for

Table 5
Distribution of elements among major species: percentage of original amount[a]

	Code	1a	2a	5a	8a	1a	2a	5a	8a
		1st stage pyrolysis 1173 K				2nd stage combustion 1298 K			
	S/Cl mole ratio	0.1228	0.1228	0.5528	0.5528	0.1228	0.1228	0.5528	0.5528
	Moles Na+K	0.0476	0.0780	0.0780	0.0476	0.0476	0.0780	0.0780	0.0476
Al	Gas	1.65E-06	1.58E-07	5.30E-08	6.04E-07	1.66E-09	6.23E-10	3.49E-10	7.55E-10
	Al in slag	55.17	63.89	100	61.36	86.34	100	100	85.60
	Stoich. solids	44.83	36.11	–	38.64	13.66	–	–	14.40
Ba	*Gas*	*0.24*	*0.24*	*0.24*	*0.24*	*0.15*	*0.07*	*0.01*	*0.02*
	Stoich. solids	*99.76*	*99.76*	*99.76*	*99.76*	*99.85*	*99.93*	*99.99*	*99.98*
C	Gas	59.42	60.95	60.78	59.31	100	100	100	100
	Stoich. solids	40.58	39.05	39.22	40.69	–	–	–	–
Ca	Gas	9.57E-04	2.21E-04	1.68E-04	4.90E-04	5.66E-05	8.85E-05	4.05E-05	3.09E-05
	Ca in slag	36.20	36.51	60.61	38.44	55.17	78.61	79.20	55.67
	Stoich. solids	63.80	63.49	39.39	61.56	44.83	21.39	20.80	44.33
Cd	Gas	100	100	100	100	100	100	100	100
Cl	Gas	100.00	53.11	57.47	100	100	100	99.85	100
	Soln-salt	2.36E-03	46.89	42.53	-	–	–	0.15	–
Cr	*Gas*	*4.42E-08*	*2.22E-08*	*1.86E-08*	*3.81E-08*	*0.0142*	*0.0088*	*0.00738*	*0.012*
	Cr in slag	*4.90E-02*	*6.87E-02*	*6.88E-02*	*5.90E-02*	*0.00934*	*0.00567*	*0.00427*	*0.00724*
	Stoich. solids	*99.95*	*99.93*	*99.93*	*99.94*	*99.98*	*99.99*	*99.99*	*99.98*
Cu	Gas	0.28	0.11	6.09E-03	1.73E-02	85.43	75.68	66.96	80.81
	Cu in slag	1.40E-02	1.62E-02	2.17E-03	1.34E-03	14.57	24.32	33.04	19.19
	Cu in matte	99.7	99.87	99.99	99.981	–	–	–	–
Fe	Gas	0.44	6.43E-02	2.66E-02	2.20E-01	2.58E-03	1.03E-03	4.79E-04	1.34E-03
	Fe in slag	0.23	0.27	0.39	0.26	0.16	0.14	0.13	0.14
	Fe in matte	1.70	1.67	28.27	28.46	–	–	–	–
	Stoich. solids	97.63	98.01	71.32	71.06	99.84	99.86	99.87	99.85
H	Gas	100	100	100	100	100	100	100	100
Hg	*Gas*	*100*	*100*	*100*	*100*	*100*	*100*	*100*	*100*
K	Gas	30.28	32.04	40.24	23.88	42.87	85.64	76.88	37.53
	K in slag	15.09	8.80	12.79	13.55	21.51	14.36	18.89	24.91
	Soln-salt	2.81E-03	58.19	46.97	–	–	–	4.24	–
	Stoich. solids	54.64	0.97	–	62.58	35.62	–	–	37.56
Mg	Gas	3.44E-03	1.48E-03	8.79E-04	2.26E-03	7.96E-04	5.63E-04	2.68E-04	4.35E-04
	Mg in slag	15.14	32.42	55.42	20.29	77.03	100	100	77.84
	Stoich. solids	84.86	67.58	44.58	79.71	22.97	–	–	22.16
N	Gas	100	100	100	100	100	100	100	100
Na	Gas	41.26	21.79	20.05	34.62	18.1	38.19	30.89	15.37
	Na in slag	58.73	34.88	52.38	65.38	81.90	61.81	65.04	84.64
	Soln-salt	4.13E-03	43.3	27.60	–	–	–	4.07	–
Ni	*Gas*	*6.37E-03*	*2.00E-03*	*1.06E-04*	*7.20E-04*	*1.03*	*0.45*	*0.18*	*0.55*
	Ni in slag	*1.12E-04*	*2.55E-04*	*6.74E-05*	*3.12E-05*	*3.21*	*2.94*	*2.55*	*2.75*
	Ni in matte	*33.93*	*32.84*	*100*	*100*	–	–	–	–
	Stoich. solids	*66.07*	*67.16*	–	–	*95.76*	*96.62*	*97.27*	*96.7*
O	Gas	85.43	87.68	87.42	85.26	96.96	97.32	97.27	96.95
	Soln-salt	1.10E-22	1.59E-17	3.83E-17		–	–	4.08E-02	–
	O in slag	7.58	6.97	10.08	8.03	1.75	1.79	1.80	1.75
	Stoich. solids	6.99	5.35	2.49	6.71	1.29	0.90	0.89	1.29
P	Gas	8.80E-04	5.88E-04	2.37E-04	8.86E-04	4.28E-09	7.68E-10	6.82E-10	3.82E-09
	P in slag	0.53	2.31	4.61	0.73	4.03	17.34	19.62	4.34
	Stoich. solids	99.47	97.69	95.40	99.27	95.97	82.66	80.38	95.66
Pb	Gas	99.34	98.93	93.49	95.41	96.84	96.50	94.20	94.77
	Pb in slag	1.30E-03	1.12E-03	1.19E-03	1.35E-03	3.16	3.50	5.80	5.24
	Pb in matte	0.66	1.07	6.51	4.59				
S	Gas	83.1940	83.4350	39.8790	39.5410	100	100	95.01	100
	Soln-salt	6.81E-21	9.80E-16	7.11E-16	–	–	–	4.99	–
	S in matte	16.81	16.57	60.12	60.46	–	–	–	
Si	Gas	1.83E-09	1.60E-09	1.17E-09	2.86E-09	1.10E-14	3.57E-15	3.06E-15	9.05E-15
	Si in slag	58.46	63.17	85.95	60.71	85.69	100	100	85.46
	Stoich. solids	41.54	36.83	14.05	39.29	14.32	–	–	14.54
Sn	*Gas*	*10.91*	*9.44*	*100*	*100*	*0.01*	*0.01*	*0.01*	*0.01*
	Stoich. solids	*89.09*	*90.56*	–	–	*99.99*	*99.99*	*99.99*	*99.99*
Ti	*Gas*	*8.91E-07*	*1.06E-07*	*7.49E-09*	*2.28E-07*	*9.30E-10*	*1.89E-10*	*6.14E-11*	*4.76E-10*
	Stoich. solids	*100*	*100*	*100*	*100*	*100*	*100*	*100*	*100*
Zn	Gas	99.19	99.09	92.09	92.55	57.80	36.40	20.54	42.16
	Zn in slag	4.89E-02	5.62E-02	8.00E-02	5.33E-02	42.20	63.60	79.46	57.84
	Zn in matte	0.76	0.85	7.83	7.40	–	–	–	–

[a] Items in italics are from the c series of calculations.

Table 6
Distribution among major species (% of original amount)[a]

Code	7a Pyrolysis	8a	2a	1a	7a Combustion	8a	2a	1a
S/Cl mole ratio	0.1228	0.1228	0.5528	0.5528	0.1228	0.1228	0.5528	0.5528
Moles Na+K	0.0476	0.0780	0.0780	0.0476	0.0476	0.0780	0.0780	0.0476
(a) Distribution of non-metallic elements								
C								
CO⟨g⟩	57.6310	59.1320	58.9540	57.5110				
CH_4⟨g⟩	1.2038	1.2082	1.2099	1.2094				
CO_2⟨g⟩	0.5811	0.6081	0.6055	0.5803	100	100	100	100
C⟨s⟩	39.8850	38.2820	38.6660	40.1870				
Fe_3C⟨s⟩	0.6939	0.7649	0.5566	0.5050				
H								
H_2⟨g⟩	95.4810	95.9440	95.9250	95.5720				
CH_4⟨g⟩	2.2801	2.2885	2.2918	2.2907				
H_2O⟨g⟩	1.2076	1.2376	1.2359	1.2095	99.1200	99.4550	99.6490	99.3720
N								
N_2⟨g⟩	99.8820	99.8820	99.8810	99.8810	99.9850	99.9840	100	99.9850
NH_3⟨g⟩	0.084316	8.4422E-02	8.4550E-02	8.4668E-02				
O								
CO⟨g⟩	81.9560	84.0900	83.8370	81.7840				
H_2O⟨g⟩	1.8133	1.8584	1.8558	1.8162	22.5380	22.6140	22.6570	22.5960
CO_2⟨g⟩	1.6527	1.7295	1.7222	1.6503	43.0700	43.0700	43.0700	43.0700
O_2⟨g⟩	3.7602E-18	3.9350E-18	3.9184E-18	3.7548E-18	31.1670	31.4460	31.0820	30.8130
Soln-salt	1.1012E-22	1.5854E-17	3.8347E-17					
O in slag	7.5781	6.9670	10.0820	8.0251	1.7513	1.7881	1.8019	1.7537
$CaAl_2Si_2O_8$⟨s⟩	1.3778	2.0616		0.84527				
$Ca_3(PO_4)_2$⟨s⟩	1.0862	1.0910	1.0654	1.2404	0.2435	0.1398	0.1360	0.24269
Fe_2O_3⟨s⟩					0.7551	0.7552	0.7773	0.75518
Mg_2SiO_4⟨s⟩								5.5788E-04
$KAlSi_2O_6$⟨s⟩	1.8128	3.2244E-02		2.0762	0.1790			0.18872
$MgOCaOSi_2O_4$⟨s⟩	2.7176	2.1641	1.4276	2.5527	0.1114			0.10578
$CaTiO_3$⟨s⟩		*1.3547*	*1.3547*		*4.6336E-02*	*2.0515E-01*	*0.2052*	*9.6776E-02*
$CaSiTiO_5$⟨s⟩	*2.2578*			*2.2578*	*0.2647*			*0.18062*
$FeCr_2O_4$⟨s⟩	*0.14261*							
$(MgO)(Cr_2O_3)$⟨s⟩		*0.2493*	*0.2493*	*0.24934*	*3.7772E-02*	*3.7776E-02*	*3.7777E-02*	*3.7774E-02*
$(NiO)(Fe_2O_3)$⟨s⟩					*2.1369E-02*	*2.1560E-02*	*2.1705E-02*	*2.1580E-02*
SnO_2⟨s⟩					*5.5157E-03*	*5.5158E-03*	*5.5159E-03*	*5.5158E-03*
$BaSO_4$⟨s⟩					*5.3513E-03*	*3.8119E-02*	*3.8144E-02*	*3.8138E-02*
$(BaO)(SiO_2)$⟨s⟩					*2.4554E-02*			
Cl								
HCl⟨g⟩	74.1180	28.4960	24.7590	71.6830	79.8010	49.2160	43.1310	76.6230
NaCl⟨g⟩	11.5760	11.5140	14.6230	13.7400	8.1908	31.5560	34.5890	9.3965
$(NaCl)_2$⟨g⟩	7.2770	7.1551	8.5647	7.6142	0.0764	1.1327	1.0087	0.0745
KCl⟨g⟩	4.4066	4.6352	7.6254	4.8126	7.1521	14.2010	17.2110	8.4569
$K(KCl)_2$	0.6772	0.7448	1.4959	0.6000	0.0434	0.1711	0.1863	0.0450
Soln-salt	0.0024	46.8910	42.5310				0.1491	
$BaCl_2$⟨s⟩	3.8154	*3.8154*	*5.1508*	*5.1509*				
S								
SO_2⟨g⟩					96.9330	96.8600	92.0030	96.9490
SO_3⟨g⟩					3.0642	3.0743	2.9039	3.0479
H_2S⟨g⟩	80.4780	80.0450	38.3080	38.2130				
COS⟨g⟩	1.4646	1.4874	0.7099	0.6933				
Soln-salt	6.8051E-21	9.7974E-16	7.1090E-16				4.9930	
Soln-matte	16.8060	16.5650	60.1210	60.4590				
$BaSO_4$⟨s⟩					*2.1837*	*15.5550*	*4.6697*	*4.6689*
P								
CHP⟨g⟩	6.1349E-04	4.3538E-04	1.7523E-04	6.1294E-04				
PN⟨g⟩	1.8348E-04	1.2293E-04	5.2285E-05	1.8323E-04				
PO_2⟨g⟩	3.5446E-08	2.1688E-08	1.0504E-08	3.5394E-08	4.2843E-09	7.6769E-10	6.8165E-10	3.8241E-09
P in slag	0.5304	2.3111	4.6051	0.7330	4.0301	17.3380	19.6160	4.3392
$Ca_3(PO_4)_2$⟨s⟩	64.8390	97.6880	95.3950	74.0440	95.9700	82.6620	80.3840	95.6610
Fe_2P⟨s⟩	34.6300			25.2230				

Table 6. Continued

Code	7a Pyrolysis	8a	2a	1a	7a Combustion	8a	2a	1a
S/Cl mole ratio	0.1228	0.1228	0.5528	0.5528	0.1228	0.1228	0.5528	0.5528
Moles Na+K	0.0476	0.0780	0.0780	0.0476	0.0476	0.0780	0.0780	0.0476
(b) Distribution of metallic elements and slag formers								
Al								
$AlCl_3$⟨g⟩	3.7459E-07	3.5324E-08	1.0944E-08	1.5587E-07	1.1415E-09	2.3971E-10	5.8316E-11	3.8045E-10
OAlOH⟨g⟩					2.8113E-10	2.5360E-10	2.3505E-10	2.6164E-10
$NaAlCl_4$⟨g⟩	5.6613E-07	5.2779E-08	1.5412E-08	2.0768E-07				
$KAlCl_4$⟨g⟩	7.1167E-07	7.0171E-08	2.6541E-08	2.4023E-07				
Al in slag	55.1720	63.8940	100	61.3580	86.3430	100	100	85.6000
$CaAl_2Si_2O_8$⟨s⟩	23.8810	35.7330		14.6510				
$KAlSi_2O_6$⟨s⟩	20.9470	0.3726		23.9910	13.6570			14.4000
Ca								
$CaCl_2$⟨g⟩	9.5666E-04	2.2067E-04	1.6816E-04	4.8969E-04	5.6517E-05	8.8263E-05	4.0245E-05	3.0809E-05
Ca in slag	36.2020	36.5100	60.6110	38.4400	55.1710	76.4760	79.1980	55.6730
$MgOCaOSi_2O_4$⟨s⟩	27.9860	22.2870	14.7020	26.2890	7.5750			7.1934
$CaAl_2Si_2O_8$⟨s⟩	10.6420	15.9230		6.5286				
$Ca_3(PO_4)_2$⟨s⟩	25.1690	63.4900	24.6870	28.7420	37.2540	21.3920	20.8020	37.1340
$CaTiO_3$⟨s⟩		*27.9020*	*27.9020*		*6.3021*	*27.9020*	*27.9020*	*13.1620*
$CaSiTiO_5$⟨s⟩	*27.9020*			*27.9020*	*21.6000*			*14.7390*
Fe								
$FeCl_2$⟨g⟩	0.4369	6.4266E-02	2.6625E-02	0.2240	2.4773E-03	9.3720E-04	3.9529E-04	1.2534E-03
Fe in slag	0.2335	0.2651	0.3920	0.2649	0.1557	0.1378	0.1265	0.1449
Fe_2O_3⟨s⟩					99.8420	99.8610	99.8730	99.8540
Fe in matte	1.7047	1.6653	28.2650	28.4560				
Fe_3C⟨s⟩	88.9120	98.0050	71.3160	64.7100				
Fe_2P⟨s⟩	8.7125			6.3457				
$NiO.Fe_2O_3$⟨s⟩					*2.1191*	*2.1381*	*2.1505*	*2.1401*
$FeCr_2O_4$⟨s⟩	*1.0708*							
K								
KCl⟨g⟩	26.2420	27.6040	33.6380	21.2300	42.593	84.5680	76.8750	37.306
$(KCl)_2$⟨g⟩	4.0330	4.4358	6.5990	2.6467	0.2587	1.0190	0.8217	0.19855
K in slag	15.0860	8.8003	12.7910	13.5470	21.512	14.3560	18.8890	37.56
$KAlSi_2O_6$⟨s⟩	54.6360	0.9718		62.5770	35.622			
Soln-salt	0.0028062	58.1880	46.9710				4.2359	
Mg								
$MgCl_2$⟨g⟩	3.4398E-03	1.4792E-03	8.7863E-04	2.2622E-03	7.7954E-04	5.3371E-04	2.3838E-04	4.1746E-04
Mg in slag	15.1370	32.4210	55.4190	20.2850	77.0300	99.9990	100	77.8420
$MgOCaOSi_2O_4$⟨s⟩	84.8600	67.5780	44.5800	79.7130	22.9690			21.8120
Mg_2SiO_4⟨s⟩								0.3451
$MgO.Cr_2O_3$⟨s⟩	*5.0005*	*11.6780*	*11.6780*	*11.6790*	*11.6830*	*11.6840*	*11.6850*	*11.6840*
Na								
NaCl⟨g⟩	25.3360	13.4390	12.6430	22.2750	17.9260	36.8330	29.9070	15.2330
$(NaCl)_2$⟨g⟩	15.9260	8.3517	7.4052	12.3440	0.1672	1.3221	0.8721	0.1208
Na in slag	58.7330	34.8800	52.3830	65.3800	81.9000	61.8080	65.0420	84.6350
Soln-salt	4.1264E-03	43.3280	27.5670				4.0717	
Si								
SiO⟨g⟩	1.8258E-09	1.0872E-09	6.6986E-10	1.6071E-09	9.1793E-15	3.4723E-15	3.0470E-15	8.6159E-15
SiS⟨g⟩	8.8537E-10	5.1163E-10	5.0360E-10	1.2315E-09				
Si in slag	58.4640	63.1690	85.9510	60.7090	85.6850	100	100	85.4610
$CaAl_2Si_2O_8$⟨s⟩	7.7146	15.2160		4.7328				
$KAlSi_2O_6$⟨s⟩	13.5330	0.3173		15.5000	8.8235			9.3035
$MgOCaOSi_2O_4$⟨s⟩	20.2880	21.2970	14.0490	19.0580	5.4914			5.2148
Mg_2SiO_4⟨s⟩								0.020627
Ti								
$TiOCl_2$⟨g⟩	*1.2047E-09*				*8.8578E-10*	*1.8479E-10*	*6.8390E-11*	*4.6437E-10*
$TiCl_3$⟨g⟩	*5.4835E-07*	*7.9053E-08*	*6.4154E-09*	*1.5964E-07*				
$TiCl_4$⟨g⟩	*3.4120E-07*	*2.7078E-08*	*1.0025E-09*	*6.7745E-08*				
$CaTiO_3$⟨s⟩		*100*	*100*		*22.5870*	*100*	*100*	*47.1740*
$CaSiTiO_5$⟨s⟩	*100*			*100*	*77.4130*			*52.8260*
Ba								
BaCl⟨g⟩								
$BaCl_2$⟨g⟩	*0.2401*	*0.2422*	*0.2410*	*0.2396*	*0.1502*	*7.2322E-02*	*8.0942E-03*	*2.4117E-02*

Table 6. Continued

Code	7a Pyrolysis	8a	2a	1a	7a Combustion	8a	2a	1a
S/Cl mole ratio	0.1228	0.1228	0.5528	0.5528	0.1228	0.1228	0.5528	0.5528
Moles Na+K	0.0476	0.0780	0.0780	0.0476	0.0476	0.0780	0.0780	0.0476
$BaCl_2$⟨s⟩	*99.7600*	*99.7580*	*99.7590*	*99.7600*				
$BaSO_4$⟨s⟩					*14.0280*	*99.9280*	*99.9930*	*99.976*
(BaO)(SiO_2)⟨s⟩					*85.8220*			
Distribution of trace elements								
Cd								
Cd⟨g⟩	100	100	100	100	67.6980	67.6000	67.7040	67.8020
CdO⟨g⟩					24.1750	24.2360	24.1400	24.0790
$Cd(OH)_2$⟨g⟩					8.1068	8.1475	8.1351	8.0987
Cr								
CrH_2O_2⟨g⟩	*6.0347E-15*	*1.4831E-08*	*1.3765E-08*	*2.4362E-08*				
$CrHO_3$⟨g⟩					*2.7678E-03*	*2.0886E-03*	*1.9810E-03*	*2.7412E-03*
CrH_2O_4⟨g⟩					*5.4730E-03*	*4.1414E-03*	*3.9227E-03*	*5.4131E-03*
Cl_2CrO_2⟨g⟩					*3.3746E-03*	*1.0598E-03*	*3.6976E-04*	*1.7278E-03*
Cr in slag	*4.9011E-02*	*6.8661E-02*	*6.8791E-02*	*5.8972E-02*	*9.3439E-03*	*5.6664E-03*	*4.2741E-03*	*7.2392E-03*
$MgO.Cr_2O_3$⟨s⟩	*42.7910*	*99.9310*	*99.9310*	*99.9410*	*99.9760*	*99.9860*	*99.9880*	*99.9810*
Cu								
CuCl⟨g⟩	0.2820	0.1011	5.9870E-03	1.7238E-02	83.5020	74.3210	66.0060	79.1590
$(CuCl)_3$⟨g⟩					1.9268	1.3561	0.9510	1.6429
Cu⟨g⟩	1.2002E-03	1.2257E-03	1.0345E-04	1.0233E-04				
Cu in slag	1.4002E-02	1.6202E-02	2.1738E-03		14.5680	24.3190	33.0390	19.1940
Cu in matte	99.7020	99.8720	99.9920					
Hg								
Hg⟨g⟩	*100*	*100*	*100*	*100*	*98.5680*	*98.6000*	*98.6230*	*98.6050*
HgS⟨g⟩	*1.1157E-04*	*1.1380E-04*	*1.5428E-04*	*1.5429E-04*				
HgO⟨g⟩					*1.3694*	*1.3742*	*1.3670*	*1.3623*
Ni								
$NiCl_2$⟨g⟩	*6.1812E-03*	*1.8948E-03*	*9.4370E-05*	*6.9005E-04*	*1.0011*	*0.4168*	*0.1539*	*0.5195*
$Ni(OH)_2$⟨g⟩					*2.8039E-02*	*2.8127E-02*	*2.8186E-02*	*2.8109E-02*
NiS⟨g⟩	*1.8250E-04*	*4.5387E-07*	*1.1094E-05*					
Ni in slag	*1.1237E-04*	*2.5490E-04*	*6.7362E-05*	*3.1218E-05*	*3.2100*	*2.9356*	*2.5521*	*2.7452*
Ni in matte	*33.9260*	*32.8390*	*100*	*99.9990*				
$NiO.Fe_2O_3$⟨s⟩					*95.7610*	*96.6190*	*97.2660*	*96.7070*
Ni_3Sn_2⟨s⟩	*66.068*	*67.1590*						
Pb								
Pb⟨g⟩	33.588	51.8550	48.8930	35.837				
PbS⟨g⟩	11.956	18.2700	27.4870	20.171				
PbCl⟨g⟩	45.596	26.9170	16.3510	34.883	1.7136	2.4022	2.8191	2.1672
$PbCl_2$⟨g⟩	8.1764	1.8458	0.7223	4.4854	86.7660	75.0100	56.9450	77.7510
PbO⟨g⟩					8.3593	19.0810	34.4210	14.8390
Pb in slag	1.3017E-03	1.1195E-03	1.1939E-03	1.3518E-03	3.1568	3.4981	5.7974	5.2354
Pb in matte	0.6550	1.0687	6.5061	4.5931				
Sn								
SnS⟨g⟩	*8.7585*	*8.7842*	*98.8890*	*92.3620*				
SnO⟨g⟩					*2.3690E-03*	*2.3632E-03*	*2.3750E-03*	*2.3811E-03*
SnO_2⟨g⟩					*1.5650E-03*	*1.5660E-03*	*1.5653E-03*	*1.5642E-03*
$Sn(OH)_2$⟨g⟩					*1.1185E-03*	*1.1185E-03*	*1.1271E-03*	*1.1276E-03*
$SnCl_2$⟨g⟩	*2.1529*	*0.6554*	*1.1087*	*7.6356*	*4.5922E-03*	*1.9060E-03*	*7.0746E-04*	*2.3966E-03*
SnO_2⟨s⟩					*99.9900*	*99.9930*	*99.9940*	*99.9930*
Ni_3Sn_2⟨s⟩	*89.0880*	*90.5600*						
Zn								
Zn⟨g⟩	85.7920	96.8810	91.2290	85.6670	5.6155E-03	9.2998E-03	1.2536E-02	8.1578E-03
$ZnCl_2$⟨g⟩	13.3990	2.2125	0.8647	6.8788	57.7910	36.3950	20.5310	42.1480
ZnS⟨g⟩	1.0749E-04	1.2015E-04	1.8052E-04	1.6972E-04				
Zn in slag	4.8879E-02	5.6193E-02	8.0011E-02	5.3289E-02	42.2030	63.5960	79.4560	57.8440
Zn in matte	0.7599	0.8499	7.8262	7.4007				

[a] Items in italics are from the c series calculations.

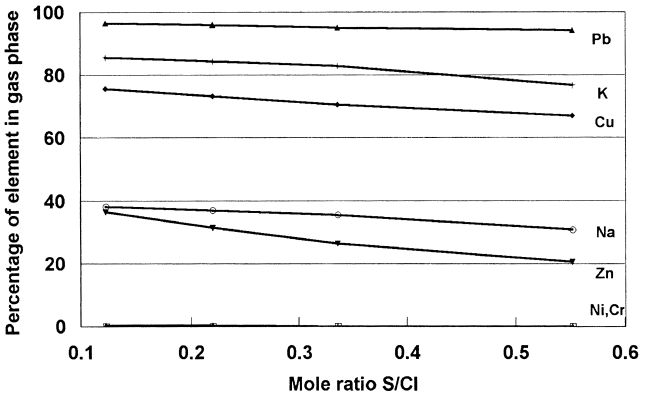

Fig. 1. Effect of S/Cl mole ratio on % trace elements in gas phase. Moles Na+K=0.078.

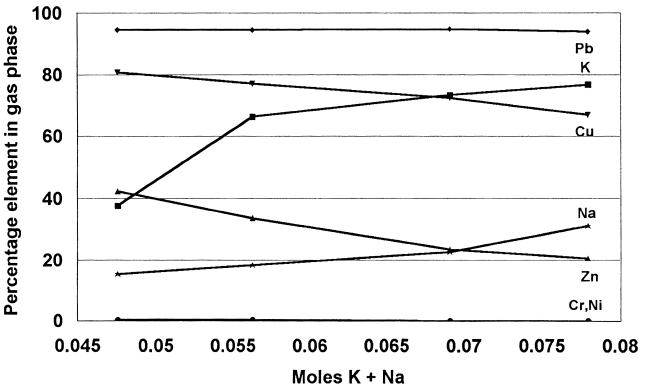

Fig. 2. Effect of alkali content on % trace element in gas phase. S/Cl mole ratio=0.5528; Ca/Si mole ratio=0.3624−0.4778.

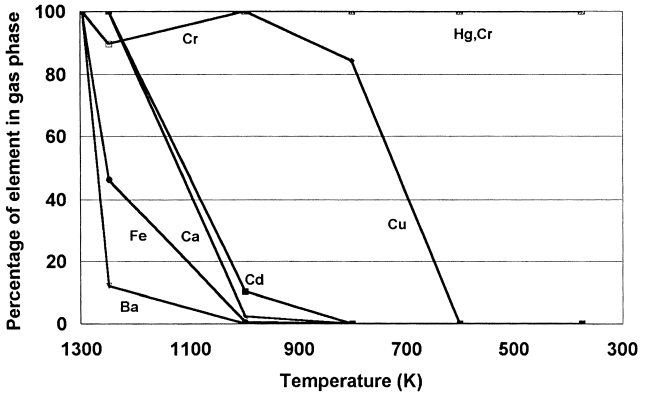

Fig. 3. Effect of cooling waste gas. Mole ratio S/Cl in original charge= 0.1228.

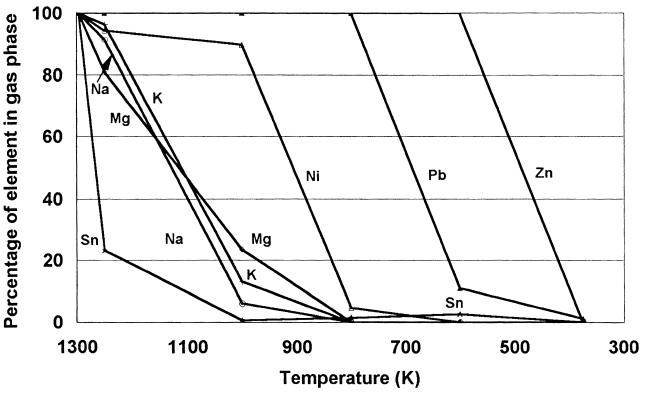

Fig. 4. Effect of cooling waste gas. Mole ratio S/Cl in original charge= 0.1228.

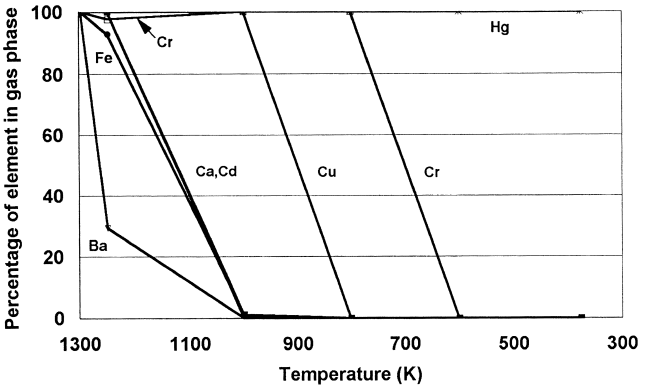

Fig. 5. Effect of cooling waste gas. Mole ratio S/Cl in original charge 0.5528.

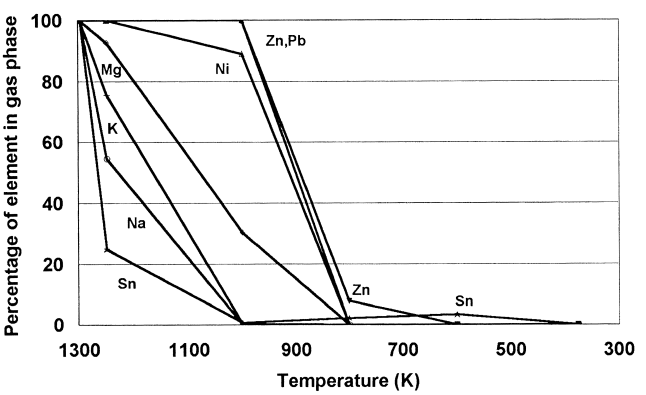

Fig. 6. Effect of cooling waste gas. Mole ratio S/Cl in original charge 0.5528.

the pyrolysis and combustion chambers and Table 7 for the cooling stages. A number of metallic elements including Fe, Ba and trace elements such as Ni, Sn and Cr remain mainly in the solid phase since only a small concentration of these metals is volatilised at 1298 K. Whilst Hg remains in the vapour phase across the whole process, Pb, Cd, Zn, Cu generally undergo the volatilisation-condensation mechanism. The presence of Cu, Pb and Zn within the slag

Table 7
Condensation sequence on cooling waste gas from 1298 K

	Code	1					2					5					8				
	Mole ratio S/Cl	0.12285					0.12285					0.55282					0.55282				
	Moles Na+K	0.04757					0.07803					0.07803					0.04757				
		Moles at temperature					Moles at temperature					Moles at temperature					Moles at temperature				
	Species	1250 K	1000 K	800 K	600 K	375 K	1250 K	1000 K	800 K	600 K	375 K	1250 K	1000 K	800 K	600 K	375 K	1250 K	1000 K	800 K	600 K	375 K
Ba	$BaSO_4$	1.920E-06	2.188E-06	2.188E-06	2.188E-06	2.188E-06	9.240E-07	1.0535E-06	1.054E-06	1.054E-06	1.054E-06	8.348K-08	1.181E-07	1.181E-07	1.181E-07	1.181E-07	3.105E-07	3.510E-07	3.510E-07	3.510E-07	3.510E-07
Ca	$CaSO_4$		2.117E-08	2.117E-08	2.117E-08	2.117E-08		3.230E-08	3.312E-08	3.312E-08	3.312E-08		1.516E-08	1.516E-08	1.516E-08	1.516E-08		1.600E-08	1.600E-08	1.600E-08	1.600E-08
Cd	CdO							3.983E-04													
	$CdSO_4$		4.199E-04	4.448E-04	4.448E-04	4.448E-04							4.391E-04	4.448E-04	4.448E-04	4.448E-04		4.416E-04	4.448E-04	4.448E-04	4.448E-04
	$CdCl_2$								4.448E-04	4.448E-04	4.448E-04										
Cr	$MgO.Cr_2O_3$						1.311E-08										1.002E-08				
	$Cr_2(SO_4)_3$				1.818E-07	2.055E-07									1.079E-07	1.082E-07				1.729E-07	1.730E-07
Cu	CuO								9.304E-05	5.945E-04											
	$CuO.CuSO_4$			2.278E-04																	
	$CuSO_4$				6.722E-04									5.264E-04	5.269E-04				6.359E-04	6.360E-04	
	$CuSO_4.H_2O$					6.722E-04					5.955E-04					5.269E-04					6.360E-04
Fe	Fe_2O_3			9.939E-07							3.948E-07	1.283E-08		1.843E-07					5.197E-07		
	$MgO.Fe_2O_3$											2.294E-09									
	$Fe_2(SO_4)_3$				9.945E-07	9.945E-07									1.846E-07	1.846E-07				5.200E-07	5.200E-07
K	K and Na salt soln	–	5.905E-03	–	–		1.314E-03	2.356E-02	2.441E-02			5.955E-03	1.505E-02					5.075E-03			
	$K_3Na(SO_4)_2$ [a]			1.827E-03	1.827E-03	1.827E-03				3.651E-03	3.651E-03			3.277E-03	3.277E-03	3.277E-03			1.600E-03	1.600E-03	1.600E-03
Mg	MgO		7.108E-08					5.324E-08	6.929E-08												
	$MgSO_4$			9.821E-08	9.821E-08					6.947E-08			2.297E-08	3.311E-08	3.311E-08			4.800E-08	5.360E-08	5.360E-08	
	$MgSO_4.H_2O$					9.821E-08					6.947E-08					3.311E-08					5.360E-08
Na	NaCl								2.096E-03	1.717E-02	1.892E-02										
	Na_2SO_4			2.236E-03	2.236E-03	2.236E-03				2.050E-03	1.176E-03			8.438E-03	8.438E-03	8.438E-03			1.875E-03	1.875E-03	1.875E-03
Ni	NiO		1.157E-06						3.214E-06												
	$NiO.Fe_2O_3$	5.716E-07	9.917E-07				2.116E-07	3.924E-07	3.946E-07	3.948E-07		–	1.824E-07				3.081E-07	5.186E-07			
	$NiSO_4$			8.766E-06	8.769E-06	8.769E-06				3.396E-06				1.676E-06	1.676E-06			7.455E-07	4.670E-06	4.670E-06	
	$NiSO_4.H_2O$										3.791E-06					1.676E-06					4.670E-06
Pb	$PbSO_4$			9.305E-04	9.348E-04	9.348E-04								9.090E-04	9.093E-04	9.093E-04			9.148E-04	9.150E-04	9.150E-04
	$PbCl_2$									8.272E-04	9.186E-04										
Sn	SnO_2	2.989E-08	4.010E-08	3.905E-08	3.847E-08	4.076E-08	2.255E-08	2.907E-08	2.882E-08	2.852E-08	2.931E-08	1.847E-08	2.441E-08	3.311E-08	2.377E-08		2.414E-08	3.131E-08	3.097E-08	3.065E-08	
	$Sn(SO_4)_2$															2.461E-08					3.150E-08
Zn	$ZnSO_4$			2.644E-04	4.419E-04									1.446E-04	1.571E-04				3.154E-04	3.220E-04	
	$ZnSO_4.H_2O$					4.419E-04					2.784E-04					1.571E-04					3.220E-04

[a] Extrapolated from 743 K.

Table 8
Analyses of salt melts formed on cooling waste gas to 1000 K

Component	Mole fraction					
Code	1	2	3	4	5	8
S/Cl mole ratio	0.12280	0.12285	0.22113	0.33650	0.55282	0.55282
Moles Na+K	0.04757	0.07803	0.07803	0.07803	0.07803	0.04757
Moles soln	0.00590	0.02356	0.01856	0.01698	0.01505	0.00507
KCl	1.63E-02	0.1742	4.97E-02	6.81E-03	3.64E-05	4.46E-03
NaCl	1.91E-02	0.4289	0.1143	1.49E-02	7.48E-03	5.00E-03
KOH	1.06E-07	2.02E-06	5.27E-07	7.42E-08	4.43E-08	3.86E-08
NaOH	1.24E-07	4.97E-06	1.21E-06	1.63E-07	9.11E-08	4.33E-08
K_2SO_4	0.44420	0.11466	0.25325	0.30633	0.32369	0.46706
Na_2SO_4	0.52043	0.28225	0.58281	0.67191	0.66519	0.52348
K_2CO_3	2.54E-10	1.73E-07	1.02E-08	1.91E-10	6.47E-11	3.25E-11
Na_2CO_3	2.97E-10	4.25E-07	2.34E-08	4.20E-10	1.33E-10	3.64E-11
KNO_3	2.66E-10	5.46E-09	1.04E-09	1.34E-10	8.15E-11	9.58E-11
$NaNO_3$	3.11E-10	1.34E-08	2.39E-09	2.95E-10	1.68E-10	1.07E-10

at 1298 K is another important prediction. A large proportion of Zn (between 42 and 79%) can be expected to be sequestered in the slag formed at combustion temperature. Smaller proportions are predicted for Cu (15–33%) and Pb (3–6%). Research carried out by Thompson and Argent [14] on trace element distributions between gaseous and condensed phases during fluidised bed gasification and combustion takes into account their solubility in slag using a series of different slag models at higher temperatures. The findings of the research show that at 1350–1500 K under combustion conditions one may expect As (70–50%), Cu (40–80%), Cr (~100%), Mn (~100%), Ni (96%) and Zn (~99%) to be found in the condensed phases whereas Pb (80–90%) will be mainly in the gas phase. These predictions are in reasonable agreement with this paper. However, because of the heterogeneity of the charge and the failure to reach equilibrium with the condensed material, more than the quoted proportions must be expected in the gas phase.

The major factors influencing the chemical form of the condensed metal phases at the surfaces of fly-ash particles are the S/Cl ratio in the waste input and to a lesser extent the sodium and potassium concentration. At high S/Cl ratio (0.5528), all condensed metals phases are sulphates (for temperatures between 800 and 375 K), except for the presence of Sn and Fe oxides. At a low S/Cl ratio (0.1228) and high alkali content, Pb and Cd chlorides prevail over sulphates at 600 and 375 K, although at lower alkali content sulphates are predicted. A combination of oxide and sulphate phases appear for nickel and copper at selected temperatures (between 800 and 375 K). Only condensed sulphate phases are present across all of the S/Cl range for Ba and Zn.

Table 9
Predicted analyses of salt melts formed on cooling waste gas

Code	2	
Temperature (K)		
Moles soln at 1000 K	1000	800
Element	1.2712E-02	1.8248E-02
	% of element in original charge	
Ca	100	100
Cu	98.10	99.99
K	18.10	90.91
Na	32.54	27.12
Pb	10.15	94.41
Zn	0.36	21.37

The total fraction of Na+K, rather than the Na/K ratio, has an effect favouring the formation of chlorides for Pb and Cd. The larger amount of Na and K attracts more sulphur, forming $K_3Na(SO_4)_2$, and therefore reduces its availability for the metals of concern. Although the majority of Ni, Cr and Ba is retained in the condensed phases during combustion the small amounts volatilised are affected by competition from the alkalis.

The results of the equilibrium calculations indicate a strong potential for a range of heavy metals (Pb, Cd, Zn, Cu) to be present at the surface of ash particles entrained in the gas phase and likely to be found in the boiler ash residues and the fly-ash particulates trapped in bag filters or an electrostatic precipitator. Formation of chloride phases will prevail at low temperatures over sulphates at low S/Cl values in the presence of high alkali contents for the toxic metals Pb and Cd. This is of importance regarding occupational exposure to contaminated dust and subsequent absorption of toxic elements in the human body as chloride compounds are known to be highly leachable and soluble particularly in acid media such as lung tissues and the gastric environment. Oxides and sulphates are formed under certain conditions, but they are less important due to their lower solubility values. Leachability tests performed on fly-ash samples in the US [9] showed that the total soluble solids varied from 0.64 to 5.32%. However, state-of-the-art waste to energy facilities met the regulatory standards and limits for critical metal concentrations in the leachates.

5. Conclusion

The predictions in this paper agree fairly well with the transport mechanisms already accepted for the major heavy metals according to their boiling points, and indicate the dissolution of some of them, principally Zn, Cu and Pb, in slag although the predicted concentrations of PbO, ZnO and Cu_2O are all less than 1 wt.%. The volatilisation–condensation mechanism prevails for the most volatile ones, in particular for Pb and Cd, and their chemical form at the surface of fly-ash particles is mainly controlled by the S/Cl ratio in the waste input. The formation of condensed cadmium and lead sulphates, dominates over the more soluble chlorides at $S/Cl \approx 0.55$ and above.

It is considered that greater attention should be paid to the possibility of trace element condensation being enhanced by solution in fused salt melts.

In global equilibrium calculations, the changing pattern of associations between compounds can be predicted but the inhomogeneous nature of the charge and the kinetic constraints are, of course, not considered. Reasonable predictions of the equilibrium concentrations of various species can be made, but sufficient time may not be available for the reaction to reach equilibrium. More attention must be paid to reaction kinetics specially in the condensation stage where temperatures are relatively low and consequently diffusion processes are slow. From a practical point of view, if the incinerator charge is made up of comparatively large discrete volumes of material (bags of paper, boxes of syringes, waste plastics), equilibrium will be difficult to achieve and it is worth examining local equilibria in areas where large pieces of waste materials, especially metals, are reacting with the surrounding environment, to predict the formation of metallic compounds and their potential to dissolve in slag melts.

Notwithstanding the above view, this study indicates that the reduction of disposable plastics, in particular PVC, in the clinical waste stream is important, firstly to avoid the presence of metals used as stabilisers such as Pb, Cd, Zn and secondly to minimise the formation of chlorides easily leachable at the surface of fly-ash particles. From an environmental point of view, the results show that the release and dispersion of dry toxic fly-ash particles in the plant or disposal in the environment warrants more concern than the presence of trace elements in the bottom ash residues where the particle sizes are larger and only a small fraction of the metals is likely to be soluble.

Acknowledgements

The authors' thanks are due to Professor A.D. Pelton and Professor C. Bale for their help in the application of FACT programs and models to this work and to Dr D. Thompson for his help in placing it in perspective relative to other combustion processes. This work was carried out through the Sheffield University Waste Incineration Centre. This paper was originally presented at The Second International Symposium on Incineration and Flue Gas Treatment Technologies, held at Sheffield University, 4–6 July 1999. It was included in the Proceedings of the Conference in the volume entitled Flue gas treatment, Session 5, 14 pp. 1999. The Proceedings were published by the Institution of Chemical Engineers and made available to participants but not given a wide circulation. The authors are grateful to the Institution for their agreement to republication in this volume. Since the paper was written, changes were made to FACT, but check calculations show that these have not significantly affected the results reported in the paper. Small changes are observed in the distribution of trace elements between the various condensed species rather than in the overall mobilisation of the trace elements.

References

[1] R.L. Davison, D.F.S. Natusch, J.R. Wallace, C.A. Evans, Trace elements in fly-ash: dependence of concentration on particle size, Environ. Sci. Technol. 8 (13) (1974) 1107–1113.
[2] C.A. Cahill, L.W. Newland, Comparative efficiencies of trace metals extraction from municipal incinerator ashes, Int. J. Envir. Anal. Chem. 11 (1982) 227–239.
[3] R.R. Greenberg, W.H. Zoller, G.E. Gordon, Composition and size distributions of particles released in refuse incineration, Environ. Sci. Technol. 12 (1978) 566–573.
[4] M.A. Fernandez, L. Martinez, M. Segarra, J.C. Garcia, F. Espiell, Behaviour of heavy metals in the combustion gases of urban waste incinerators, Environ. Sci. Technol. 26 (5) (1992) 1040–1047.
[5] C.Y. Wu, P. Biswas, An equilibrium analysis to determine the speciation of metals in an incinerator, Combust. Flame 93 (1993) 31–40.
[6] T.T. Eighmy, J.D. Eusden, J.E. Krazanowski, D.S. Domingo, D. Stampfli, J.R. Martin, P.M. Erickson, Comprehensive approach toward understanding element speciation and leaching behavior in municipal solid waste incineration electrostatic precipitator ash, Environ. Sci. Technol. 96 (3) (1995) 629–646.
[7] T. Hundesrugge, K.H. Nistsch, W. Rammensee, P. Schoner, Mull Abfall 6 (1989) 318–324.
[8] J.L. Ontiveros, T.L. Clapp, D.S. Kosson, Physical properties and chemical species distributions within municipal waste combustion ashes, Environ. Prog. 8 (3) (1989) 200–206.
[9] NUS, EPA/530-SW-90-029A, NTIS PB90-187154, Characterization of MCW ash, ash extracts and leachates, Coalition on Resource Recovery and the Environment, US EPA Office of Solid Waste, Washington, DC, 1987.
[10] J.F. Sandell, G.R. Dewey, L.L. Sutter, J.A. Willemin, Evaluation of lead-bearing phases in municipal waste combustor fly ash, J. Environ. Eng. 122 (1) (1996) 34–40.
[11] F. Hasselriis, Relationship between input and output, in: A. Green (Ed.), Medical Waste Incineration and Pollution Prevention, Van Nostrand Reinhold, New York, 1992.
[12] F. Hasselriis, L. Constantine, Characterisation of today's medical waste, in: A. Green (Ed.), Medical Waste Incineration and Pollution Prevention, Van Nostrand Reinhold, New York, 1992.
[13] C.W. Bale, A.D. Pelton, École Polytechnique de Montréal, Montréal, Québec, Canada, February 1999 (http://www.crct.polymtl.ca).
[14] D. Thompson, B.B. Argent, The use of Thermodynamic Computation Packages to Predict the Reactions Occurring during Combustion and Gasification in Fluidised Beds, 3rd International Conference on Combustion Technologies for a Clean Environment, Lisbon, Portugal, 1995, July.
[15] J. Lumsden, Thermodynamics of Molten Salt Mixtures, Academic Press, London, UK, 1966.